Short-term pre-operative dietary restriction in vascular surgery

Kip, P.

Chapter 4.

Short-Term Pre-Operative Methionine Restriction Protects from Vascular Wall Maladaptation Via PVAT Dependent Mechanisms.

Peter Kip[1, 2, 3], Thijs J Sluiter[1,2,3], Michael R MacArthur[2], Ming Tao[1], Jonathan Jung[2,4], Sarah J Mitchell[2], Josh Gorham[5], John Seidman[5], Paul H.A. Quax[3], C. Keith Ozaki[1], James R Mitchell[2,6] & Margreet R de Vries[3]

[1] Department of Surgery and the Heart and Vascular Center, Brigham & Women's Hospital and Harvard Medical School, Boston, MA, 02115 USA.

[2] Department of Molecular Metabolism, Harvard T.H. Chan School of Public Health, Boston, MA, 02115 USA.

[3] Einthoven Laboratory for Experimental Vascular Medicine and Department of Surgery, Leiden University Medical Center, Leiden, the Netherlands.

[4] School of Medicine, University of Glasgow, Glasgow, UK.

[5] Harvard Medical School, Boston MA 02115 USA.

[6] Department of Health Sciences and Technology, ETH Zurich, Switzerland.

Abstract.

Rationale: All (cardio)vascular procedures involve peri-operative manipulation of adipose tissue, either subcutaneous or perivascular (PVAT), while a "sick fat" phenotype is detrimental to surgical outcome. Short-term preoperative methionine restriction (MetR) shows promise as a novel strategy to alter the response to surgical injury, but its effects in arterial and vein graft intimal hyperplasia (IH) are unknown.

Objective: We hypothesized that short-term MetR can attenuate IH after arterial injury and vein graft surgery, and that these benefits are PVAT-dependent.

Methods and Results: Mice (C57BL/6 male, 12-weeks) consumed a high-fat diet (Control; 0.6% methionine/60% fat) for 3-weeks. Half were switched to a 1-week MetR diet (0.05% methionine/60% fat) while the control group remained on control-diet. One cohort from both diet groups underwent carotid artery focal stenosis. Donor-animal vena cava (VC) PVAT was either partially stripped, completely stripped (-PVAT) or left intact (+PVAT), then carotid-interposition grafting into diet-matched recipients was performed. Immediately post-op, all mice were control-fed. At post-op day (POD) 28, grafts and carotid arteries were harvested for histology and immunohistochemistry. Pre-op (VC, aorta [AO]) and vein graft POD1 PVAT were processed for RNA-sequencing.

Results: Short-term MetR attenuated intima/media-area ratios after focal stenosis. In vein grafts, protection was dependent on diet-PVAT interactions, with a 53.3% decrease in intima/media+adventitia-area ratios in the MetR +PVAT group, compared Control +PVAT. MetR +PVAT vein grafts had a 59.1% reduction in intimal M1/M2 ratios, compared to Control +PVAT, and this was also dependent on diet-PVAT interaction. MetR increased thermogenesis in arterial-, and AMPK-signaling in arterial and venous PVAT. At POD1 MetR downregulated the pro-inflammatory ligand tenascin-c and anti-atherosclerotic enzyme lysyl-oxidase.

Conclusions: Short-term preoperative MetR attenuated arterial and vein graft IH, and in vein grafts this was PVAT dependent. Mechanistically, MetR induced browning and increased AMPK-signaling in PVAT at baseline, while dampening the post-operative pro-inflammatory response to the surgery.

1. Introduction.

With more than 1 million inpatient (lower extremity) vascular procedures[1] and 150,000 coronary artery bypasses performed annually in the US alone[2], revascularization surgery remains a mainstay in the treatment of arterial occlusive disease. These interventions, however, are hampered by high failure rates. One-year primary patency after lower extremity balloon angioplasty, for example, ranges between 31-55%.[3, 4] And while venous bypasses of the coronary artery have a one-year primary patency of 76%[5], in the lower extremity this falls towards 60%.[6]

The mid- to long-term failure of an initial successful vascular procedure originates from accelerated intimal hyperplasia (IH).[7] This pathophysiological response to surgical injury as in balloon angioplasty, or altered hemodynamics as in vein grafting, is defined by initial endothelial dysfunction and leukocyte transmigration.[7, 8] This in turn triggers vascular smooth muscle cell (VSMC) migration and proliferation and ultimately occludes the artery or vein graft.[7, 9] And despite decades of research, therapies to limit this remodeling response of the vascular wall after a (cardio)vascular intervention are not available.

In addition to the interaction between systemic inflammation and the cellular composition of the vascular wall, perivascular adipose tissue (PVAT) surrounding the vessel also functions as a paracrine organ with the potential for impacting vascular vessel patency following an intervention.[10, 11] Interestingly, in the context of obesity and subsequent inflamed PVAT, preclinical work suggests that this can accelerate IH.[11] For example, high-fat feeding (HFD) in rodents increases the secretion of interleukin-6, interleukin-8 and monocyte chemoattractant protein-1 (MCP-1) from perivascular adipocytes.[12] A comparable diet triggered the infiltration of pro-inflammatory monocytes in visceral adipose tissue which was then transplanted onto the carotid artery, as a surrogate for the presence of inflamed PVAT pre-surgery. After carotid wire injury, cohorts who received inflamed adipose tissue had exacerbated neointima formation.[13] In a comparable study, aorta PVAT transplantation onto the carotid artery from HFD-induced obese mice also accelerated neointima formation subsequent to carotid wire injury.[14] Switching from a HFD to normal chow can also rapidly alter fat phenotype[15], but the functional relevance of this in terms of protection against IH as well as a underlying mechanism of action remain uncharacterized.

Surgical trauma to the fat itself can also alter its local phenotype and even yield a systemic response. For example, mechanical injury to subcutaneous adipose tissue triggered local production of interleukin-6 and interleukin-1β (IL-1β).[16] In a separate study, a comparable surgical injury to the fat elicited increased levels of circulating interleukin-6, and this response was exacerbated in obese patients.[17] In a preclinical model of surgical injury to the adipose tissue, unilateral surgical trauma to inguinal adipose induces local and distant browning[15], but whether this could be beneficial in post-operative recovery is unknown.

In this same surgical trauma model, the authors lowered the high-fat content of the diet to normal levels for the 3-weeks leading up to the surgical injury. Interestingly, this short-term change in dietary intake not only reduced baseline adipose levels of MC-1 and tissue necrosis factor-α (TNF-α), but it also altered the response of the fat to surgical trauma. At post-op day (POD) 1, local levels of both IL-1β and TNF-α where reduced compared to mice who received a preoperative high-fat diet.[18] Which pathways are activated due to such a short-term change in dietary intake, and whether this protection could extend to PVAT in vascular injury models, has not been investigated.

This concept of utilizing short-term dietary interventions before surgery to precondition the body, in order to alter the host's response to surgical injury, stands as an emerging approach to enhance surgical outcomes.[19, 20] Dietary restriction (DR), defined as restriction of either total calories, macronutrients such as protein or specific essential amino acids without malnutrition, during the preoperative time period of days to weeks represents one such dietary preconditioning approach.[20, 21] Efficacy of these short-term diets has been shown in a wide range of preclinical surgical models, including renal[19, 22, 23], hepatic[19, 24, 25] and vascular injury models.[26] Recently, we reported that short-term restriction of dietary protein intake attenuates IH and subsequent vein graft disease (VGD) in a venous bypass graft model, potentially via impaired VSMC migration.[27]

Methionine restriction (MetR) is a DR regimen in which dietary sulfur amino acid (methionine and cysteine) content, but not overall calorie intake, is reduced. In rodents, MetR has pleiotropic beneficial effects on markers of cardiometabolic health[28] and lifespan[29] likely via effects on adipose tissue[30] and energy metabolism[31], while specifically in surgical models MetR improves outcome of femoral ligation by increasing angiogenic potential[32] and preserves wound healing[33]. In humans, MetR delivered for up to 16 weeks as a semi-synthetic diet is feasible and increases fat oxidation and reduces intrahepatic lipid content.[34]

Here we tested the hypothesis that short-term pre-operative MetR can attenuate IH in models of either arterial injury or VGD specifically through interaction with PVAT, with implications for dietary preconditioning in human vascular injury. Mechanistically, we evaluated changes in PVAT gene expression prior to and after surgery and their modulation by MetR.

2. Methods.

2.1 Experimental animals.

All animal experiments were approved by the appropriate Harvard Medical Area or Brigham and Women's Hospital Institutional Animal Care and Use Committee () and in accordance with the NIH guidelines. All surgical experiments were performed on C57BL/6 mice (male, 14-16 weeks old, Stock No: 000664, Jackson Laboratory). Mice were housed 4-5 per cage and maintained on a 12-hour light-dark cycle at 22°C with 30-50% humidity.

2.2 Dietary Intervention.

All mice (aged 10-12 weeks old) were started on a 3-week 60% fat (by calories), 0% cysteine diet (Research Diets, A18013001) [Control] which contained standard levels of methionine (0.64%, 2.6% of total protein)., (**Fig. S1A**) After 3 weeks of Control diet, 1 cohort was switched to a methionine restriction (MetR) diet containing 60% fat, 0% cysteine and 0.07% methionine0.3% of total protein) [Research Diets, A18022602]. (**Fig. S1A**) After 1 week of MetR or continued Control diet, mice were either harvested for caval vein /baseline studies or underwent a surgical intervention (see below for description of vein graft surgery and focal stenosis creation. Immediately post-operatively, all mice were switched back to the Control diet and harvested at either post-op day 1 (POD1) or post-op day 28 (POD28). Mice subjected to MetR lost approximately 20% of their starting weight (**Fig. 1SB,** representative weight curve), despite hyperphagia during the dietary intervention (**Fig. S1C**), but regained weight rapidly post-operative (**Fig. 1SB**).

2.3 Focal Stenosis Creation.

A focal stenosis was created as described previously to generate an arterial intimal hyperplastic response.[35] Mice were anesthetized with isoflurane and the right common carotid artery (RCCA) was dissected from its surrounding tissue. A 35-gauge blunt needle mandrel was then placed longitudinally along the RCCA and tied with a 9-0 nylon suture approximately 2-2.5mm proximal to the bifurcation. After removal of the needle mandrel, the skin was closed with a 6-0 Vicryl suture. Post-operatively mice received warm lactate ringer solution (0.5mL, subcutaneous) and buprenorphine (0.1mg/kg, subcutaneous).

2.4 Vein Graft Surgery.

Vein graft surgery was performed as described previously. [36] In brief, anesthesia was induced via a nose cone with 5% isoflurane and maintained under 2-3% for the duration of the procedure. Shortly before the start of the recipient surgical procedure, the thoracic caval vein of a donor mouse was harvested and placed in ice-cold sterile 0.9% NaCl supplemented with heparin (100UI/mL). In the recipient, neck region fur was removed, and a neckline incision was performed. The right common carotid artery (RCCA) was dissected from its surrounding soft tissues and 2 8-0 nylon sutures were tied in the middle, approximately 1mm apart. RCCA was then cut between the two sutures to facilitate an end-to-end anastomosis. The proximal and distal RCCA was then everted over an autoclavable nylon cuff (Portex) of approximately 2mm while clamped with vascular clamps. The everted carotid walls were secured with an 8-0 nylon suture. Next the donor caval vein was sleeved between both RCCA ends, and an end-to-end anastomosis was created with 8-0 nylon sutures. The distal followed by the proximal vascular clamp was released to restore blood flow. The incision was closed with 6-0 Vicryl sutures. Post-operatively animals received warm lactate ringer solution (0.5mL, subcutaneous) and buprenorphine (0.1mg/kg, subcutaneous).

2.5 Vein Graft PVAT Manipulation.

In routine rodent vein graft surgery[36], as well as in our first cohort of vein graft dietary intervention experiments, the donor caval vein was partially trimmed of its surrounding PVAT to facilitate ~~technically straightforward~~ end-to-end anastomosis creation in the recipient. In a follow-up cohort of C57BL/6, we either completely stripped the donor caval vein of its surrounding PVAT or left all PVAT intact. The donor caval vein (with/without PVAT) was then transplanted into a recipient RCCA on a corresponding diet (Control-fed or MetR), to create a vein graft with PVAT intact, or a vein graft lacking PVAT. This resulted in 4 separate groups evaluating the interplay of diet and the presence of PVAT around the vein graft: Control – PVAT, Control + PVAT, MetR – Control, MetR + PVAT. Stripped donor caval vein PVAT was collected on dry ice, snap frozen in liquid nitrogen and then stored at -80°C for subsequent analyses.

2.6 Vein graft/RCCA POD28 Harvest.

Mice were exsanguinated under anesthesia, followed by insertion of a 21G needle in the left ventricle. Whole-body perfusion was performed with lactate Ringers solution for 3 minutes, then switched to 3 minutes of perfusion-fixation with 10% formalin. The graft/RCCA was excised en-bloc via a midline neck incision and transferred to a 10% formalin (in PBS) solution for 24 hours. After 24 hours the tissue was transferred to a 70% ethanol solution for further processing.

2.7 Baseline Studies.

To study effects of diet without surgery, baseline data was secured from mice fed an identical dietary intervention (3-week control diet followed by 1-week MetR or control) and harvested after 1 week of MetR/control. All tissue was collected on dry ice and snap frozen in liquid nitrogen, before storage at -80°C. For baseline harvest, mice were first anesthetized, and a cardiac puncture was performed to collect 1mL of whole blood in a 1.5mL ethylenediaminetetraacetic acid (EDTA)-coated Eppendorf for downstream blood analysis. A thoracotomy was performed and caval vein PVAT was carefully dissected from the vessel wall with forceps. The caval vein was then harvested and caval vein wall and PVAT were stored separately. Lungs and heart were removed and thoracic aorta PVAT was carefully separated from the vessel wall, followed by harvest of the aortic wall. Both aorta and aorta PVAT were stored separately.

2.8 Vein Graft POD1 Harvest.

For vein graft POD1 harvest, after mice were anesthetized, the neck suture was removed and the surgical field from the previous day was opened. Vein graft patency was first ensured. In one cohort of mice, 1mL whole blood was collected via cardiac puncture in an EDTA-coated Eppendorf for downstream whole-blood analysis, and then the vein graft was removed for histology as follows. A thoracotomy was performed, followed by whole-body perfusion via the left ventricle with ringer's lactate solution. A 21G syringe containing O.C.T. (Tissue-Tek, # 25608-930) was carefully inserted in the brachiocephalic trunk oriented towards the RCCA. Next, O.C.T. was slowly released into the

brachiocephalic trunk until the vein graft started to dilate. After placing an 8/0 suture around the distal cuff, it was tightened followed by a second suture around the proximal cuff. The now dilated vein graft was removed en-bloc and placed in a mold filled with O.C.T., then placed on dry ice and stored in -80°C. In a second cohort of mice, the PVAT surrounding the vein graft was carefully removed using forceps and collected in a 1.5mL Eppendorf on dry ice. Next, the vein graft wall itself was taken out and collected in a separate Eppendorf on dry ice. Both PVAT and vein graft were then snap frozen in liquid nitrogen and stored at -80°C.

2.9 Vein Graft/RCCA Histology.

POD28 Vein grafts and RCCA (at POD28 after focal stenosis surgery) were harvested, embedded in paraffin and cut in 5µm sections by microtome, then mounted on slides. Grafts were sectioned at regular intervals of 200 µm, starting from the proximal cuff till 1000µm post proximal cuff. Focal stenosis arteries were cut at regular intervals of 400µm, starting at 400µm proximal from the focal stenosis, until 2800µm proximal from the stenosis. For histomorphometric analysis, a Masson-Trichome staining was performed: after deparaffinization to 95% ethanol, slides were immersed in 5% picric acid (in 95% ethanol) for 3 minutes, followed by a 3-minute stain in working Harris Hematoxylin Solution (Fisher 213 Scientific, cat# 245-678). After a brief tap water wash, slides were stained with 1% Biebrich Scarlet in 1% acetic acid (Fisher Scientific, cat# A38S-500) for 3 minutes, followed by a quick rinse in distilled water. Slides were then stained for 1 minute in 5% Phosphomolybdic/Phosphotungstic acid solution and immediately transferred to 2.5% light green SF yellowish in 2.5% acetic acid (Fisher Scientific, cat# A38S-500) for 4 minutes. Followed by a quick rinse in distilled water and a 2-minute rinse in1% acetic acid solution (Fisher Scientific, cat# A38S-500). After dehydration with Xylene slides were covered with a cover glass employing Permount (Electron Microscopy Science, cat# 17986-05). Brightfield images of vein graft and carotid artery cross-sections were taken with a Zeiss Axio A1 microscope (Carl Zeiss). Histomorphometric analysis was performed using Image J 1.51p (Java 1.8.0_66) (see below).

2.10 Histomorphometric Analysis.

For vein graft histomorphometric analysis, images of cross sections taken at 200µm, 400µm, 600µm, 800µm and 1200µm post-cuff were uploaded in ImageJ. Per distance, 1 cross section was analyzed. Area and perimeter of lumen, internal elastic lamina and adventitial border were measured in $\mu m^2/\mu m$. Next, lumen area, intimal area, intimal thickness, media+adventitia (M+A) area, M+A thickness, intimal/media+adventitia (I/M+A) area ratio and I/M+A thickness were calculated as described previously.[37] 200µm-1000µm cross sections were next averaged into a per-vein graft histomorphometric endpoint. For focal stenosis histomorphometric analysis, RCCA cross section images taken at 400µm, 800µm, 1200µm, 1600µm and 2000µm proximal from the focal stenosis were uploaded in ImageJ. Lumen area and perimeter, internal elastic lamina area and perimeter, external elastic lamina area and perimeter were measured. Next, lumen area, intimal area and thickness, medial area and thickness and I/M area and thickness ratios were calculated. Collagen measurements were performed via the color deconvolution function in ImageJ, the resulting split green area was measured via pixel-threshold and normalized to total intimal/M+A and total vein graft area in %.

2.11 Immunohistochemistry.

First, vein graft slides were incubated for 30' at 60°C in a vacuum oven, followed by immediate deparaffinization. Next, antigen retrieval was performed for 30' at 97°C in Citrate buffer (pH 6.0, in PBS) [Abcam, ab93678]. Then, slides were pre-incubated with 10% goat serum (Life Technologies, 50062Z) in PBS with 0.3M Glycine (Aijomoto, R015N0080039) for 1hr at room temperature (RT). Slides were then incubated with primary antibodies. For VSMC+KI-67 double-staining: SMC-α (mouse anti-mouse, Abcam, ab7817, 1:800) and Ki-67 (rabbit anti-mouse, Abcam, ab16667, 1:100) o/n at 4°C. For M1/M2 macrophage staining, 1 vein graft slide containing 2-4 cross sections was double stained with the general macrophage marker Mac-3 (rat anti-mouse, Fisher Scientific, B550292, 1:600) and either iNOS (rabbit anti-mouse, abcam, ab3523, 1:100) for M1, or CD206 (rabbit anti-mouse, abcam, ab64693, 1:800) for M2. Slides with primary antibodies were incubated o/n at 4°C. Slides were then washed in PBS + tween (PBST) and incubated in secondary antibody for 2hrs at RT. For SMC-α + Ki-67 double staining, slides were incubated with Alexa Fluor 647 (goat anti-mouse, A-32728) and Alexa Flour 568 (goat anti-rabbit, A-11011) at 1:600. For M1/M2 staining, slides were incubated with Alexa Fluor 568 (goat anti-rabbit, A-11011) and Alexa Fluor 647 (goat anti-rat, A-21247) at 1:600. After secondary antibody incubation, slides were washed in PBST and mounted with DAPI (Vector, CB-1000) or stained with Hoechst staining solution and mounted with anti-fade as indicated.

2.12 Immunohistochemical analysis.

For fluorescent IHC, 20x images were taken with a Laser Scanning Confocal Microscope (Zeiss LSM800) and automatically stitched. For non-fluorescent IHC, 10x brightfield images were taken with a Zeiss Axio A1 microscope (Carl Zeiss)

and stitched with Adobe Photoshop. Lumen area, intimal area, M+A area and PVAT area were defined and measured in ImageJ, based on the corresponding Masson-trichome histology picture. For VSMC + Ki-67 double staining analysis, 1 cross section per vein graft was analyzed (600 or 800µm). Based on Hoechst/DAPI stain the lumen, intima and M+A area was measured in mm^2. The SMC-α positive fluorescent (647nm) channel was analyzed for total SMC-α positive pixels via color-threshold and then normalized to its respective vein graft layer (intima, M+A or total vein graft) in %. A cell positive for both SMC-α and Ki-67 was regarded as a "proliferating VSMC". Total proliferating VSMCs per vein graft layer were then counted and normalized to cells/mm^2. Total SMC-α positive cells were counted per vein graft layer and normalized to VSMC/mm^2 per vein graft layer. For analysis of macrophage polarization, one slide per vein graft (at 800µm) containing 2-4 cross sections was stained with Mac-3+iNOS or Mac-3+CD206. Lumen area, intimal area, M+A area and PVAT area were measured in mm^2. All cells positive for Mac-3 were determined macrophages (M_θ). Cells positive for Mac-3 and iNOS: M_1-macrophage. Cells positive for Mac-3 and CD206: M_2-macrophage. In each cross section the total number of M_θ and M_1 or M_2-macrophages per vein graft layer was counted and normalized to mm^2. Per vein graft layer, M_1 and M_2-macrophages (in count per mm^2) were normalized as a percentage of the total M_θ-macrophages present in that layer (also in count/mm^2). The resulting M_1 and M_2-macrophage percentages were then used to calculate a M_1/M_2 ratio.

2.13 Duplex ultrasound biomicroscopy

In both MetR and control-fed mice subjected to vein graft surgery with/without PVAT, high resolution ultrasonography was performed at POD14 and POD28. A Vevo 2100 imaging system with 18- to 70-MHz linear array transducers (Visual Sonics Inc., Toronto, ON, Canada) was employed to measure vein graft lumen diameters. Mice were anaesthetized with 2-3% isoflurane and body temperatures were maintained at 37°C using a heated stage. M-mode was used for vessel cross-sectional dimensions. Three luminal axial images were performed (proximal, distal, and mid vein graft), and mean vessel luminal diameters were calculated.

2.14 RNA isolation from adipose tissue & primary cells.

Adipose tissue samples were collected on dry ice, snap frozen in liquid nitrogen and stored at -80°C. For RNA sequencing analysis of aorta (arterial) PVAT, the aorta PVAT of two mice on corresponding diets was pooled in one pre-cooled Eppendorf on dry ice. For caval vein and vein graft PVAT RNA sequencing, PVAT from 3 mice on corresponding diets was pooled in one pre-cooled Eppendorf on dry ice. Next, 250 µL Trizol (Thermo Fisher, cat# 15596026) was added per Eppendorf and the tissue was thoroughly homogenized with a hand-held tissue homogenizer. After homogenization, samples were centrifuged at 12.000x*g*, 5 min at 4°C. Supernatant was transfer to a fresh tube and incubated for 5' at RT, then 200µL of chloroform (Sigma-Aldrich, cat#288306-1L) was added and the tube incubated for 2' on wet ice. After centrifuging tubes at 12.000x*g* for 10' at 4°C, the aqueous layer was collected on a fresh tube on ice. 250µL iso-propanol and 1µL glycogen was added to each sample, vortexed and centrifuged (12.000x*g*, 10' at 4°C). Supernatant was aspirated and 75% EtOH was added before Eppendorf was vortexed and centrifuged (12.000x*g*, 10' at 4°C). This EtOH wash was repeated for a total of three times, then the RNA-pellet was left to dry for 20' at RT. Pellet was then eluted in 20µL of RNAase free H_2O and stored at -80°C.

2.15 Statistical analysis.

All data are expressed as mean ± standard deviation unless indicated otherwise. Normality testing was performed employing the Shapiro-Wilk normality test. Normally distributed data was analyzed by Student's *t*-test or two-way ANOVA. Non-normally distributed data was analyzed by Mann-Whitney test. All testing was done via Graphpad Prism (8.4.2).

3. Results.

3.1 Short-term MetR improves both arterial and vein graft revascularization strategies.

We first examined whether MetR was able to attenuate negative wall remodeling after an intimal hyperplasia-inducing hemodynamic vascular procedure by creating a focal stenosis of the RCCA in short-term MetR (and control) mice. **Fig. 1A** outlines the experimental design of all *in-vivo* dietary experiments. **Fig. 1B** outlines the focal stenosis creation, resulting in arterial intimal hyperplasia and remodeling along the RCCA. At day 28 post-op, the RCCA was harvested and processed for histology (**Fig. 1C**). Interestingly, mice preconditioned with MetR had no detectable arterial intimal hyperplasia at POD28, while control-fed mice displayed increased I/M area ratios at 400µM post-stenosis (**Fig. 1D**).

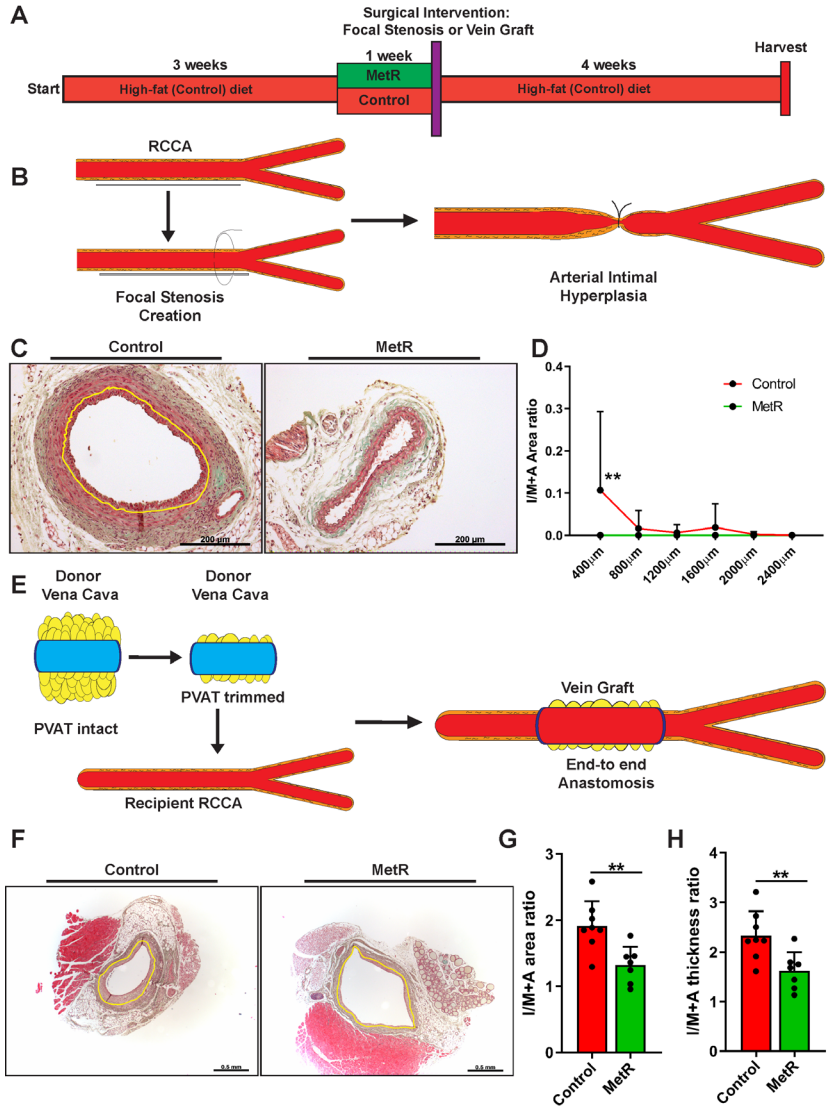

Figure 1. Short-term MetR improves both arterial and vein graft revascularization strategies. A: schematic of dietary intervention. **B:** focal stenosis creation. **C**: RCCA at POD28 after Masson-trichome staining. Yellow line indicates internal elastic lamina lining. Scale bars = 200µm. **D:** I/M area ratio at POD28, via Two-way ANOVA with Sidak's multiple comparisons test, n=8-9/group. **E:** vein graft surgery procedure, with partial trimming of PVAT from donor vena ceva. **F**: vein grafts at POD28 after Masson-trichome staining. Yellow lining indicates internal elastic lamina. Scale bars = 0.5mm. **G**: I/M+A area ratio with Student's t-test, n=7-8/group. **H**: I/M+A thickness ratio with Student's t-test, n=7-8/group. ** P<0.01

We next explored whether vein graft durability could benefit from MetR preceding bypass surgery. **Fig. 1E** outlines the vein graft surgical procedure, as performed routinely[36], which includes partial stripping of caval vein PVAT to better facilitate anastomosis in the recipient.[38] Caval veins from donor mice where then implanted in recipients (on a corresponding diet) via an end-to-end anastomosis. At POD28, vein grafts were harvested and processed for histology (**Fig. 1F**). After morphometric analysis, pre-operative MetR mice had a significant decrease of 31% and 30.5% in I/M+A area (**Fig. 1G**) and thickness (**Fig. 1H**) ratios respectively.

Taken together, these data show that short-term pre-operative MetR can mitigate both the arterial intimal hyperplastic response and vein graft disease after bypass surgery.

3.2 Protection from Vein Graft Disease via Short-term Methionine Restriction is Perivascular Adipose Tissue Dependent.

We next sought to better understand the mechanism by which MetR protects against IH. Considering the potential of perivascular fat to modify surgical outcome[10, 11], together with the published effects of MetR on different adipose depots[30], we hypothesized that protection from VGD by short-term MetR is dependent on modulation of local PVAT phenotype. **Fig. 2A** depicts the experimental design to test this, with the donor vena cava either completely stripped of its PVAT ("No PVAT") or with PVAT left intact ("PVAT"). The vena cava is then transplanted into a recipient on a corresponding diet (Control or MetR), creating a vein graft with or without PVAT (**Fig. 2A-B**) or completely intact (**Fig. 2C-D**). At POD28, grafts were harvested and processed for histology (**Fig. 2E**). Histomorphometric analysis revealed a PVAT-dependent protection from vein graft disease by MetR, as demonstrated by a significant decrease in I/M+A area ratios (53.3% ,**Fig. 2F**), and I/M+A thickness ratios (53.5%, **Fig. 2G**) compared to Control + PVAT; while there was no difference between diet groups without PVAT. Furthermore, two-way ANOVA analysis established a signification diet-PVAT interaction in both vein graft layer thickness and area ratios (**Fig. 2H-I**). MetR + PVAT vein grafts trended towards a smaller intimal area (**Fig. S2A**) but had no change in intimal thickness (**Fig. S2B**). At POD28, lumen area was decreased in MetR + PVAT mice (**Fig. S2C)**, which was confirmed by ultrasound analysis (**Fig. S2D**). Although this also revealed that MetR vein grafts appeared to decrease in lumen diameter at a lesser rate between POD14 and 28 (**Fig. S2D**). The favorable morphology of MetR + PVAT vein grafts was mainly driven by an increase in M+A thickness, (37%, **Fig. 2G**) and area (27.1%, **Fig. 2H**).

Table 1. Percentage of variation between groups that can be explained by diet, PVAT or a diet-PVAT interaction. Two-way ANOVA with Tukey's multiple comparison test on histomorphometric parameters in **Figure 2** & **Fig. S2.** n=11-13/group.

Histomorphometric parameter	Source of Variation	% of total variation	P-value	P-value summary
	Interaction	9.146	0.0146	*
I/M+A area ratio	PVAT +/-	0.006033	0.9482	ns
(Fig. 2F)	Diet	31.16	<0.0001	****
	Interaction	7.538	0.0324	*
I/M+A thickness ratio	PVAT +/-	0.001153	0.9783	ns
(Fig. 2G)	Diet	24.40	0.0003	***
	Interaction	4.274	0.1451	ns
Intimal area	PVAT +/-	0.3439	0.6760	ns
(Fig. S2A)	Diet	10.96	0.0219	*
	Interaction	2.284	0.2734	ns
M+A area	PVAT +/-	0.4127	0.6397	ns
(Fig. 2I)	Diet	16.50	0.0047	**
	Interaction	2.507	0.2736	ns
Intimal thickness	PVAT +/-	1.591	0.3819	ns
(Fig. S2B)	Diet	6.780	0.0751	ns
	Interaction	8.223	0.0159	*
M+A thickness	PVAT +/-	1.254	0.3325	ns
(Fig. 2H)	Diet	35.61	<0.0001	****
	Interaction	6.514	0.0719	ns
Lumen area	PVAT +/-	0.2124	0.7407	ns
(Fig. S2C)	Diet	10.26	0.0253	*

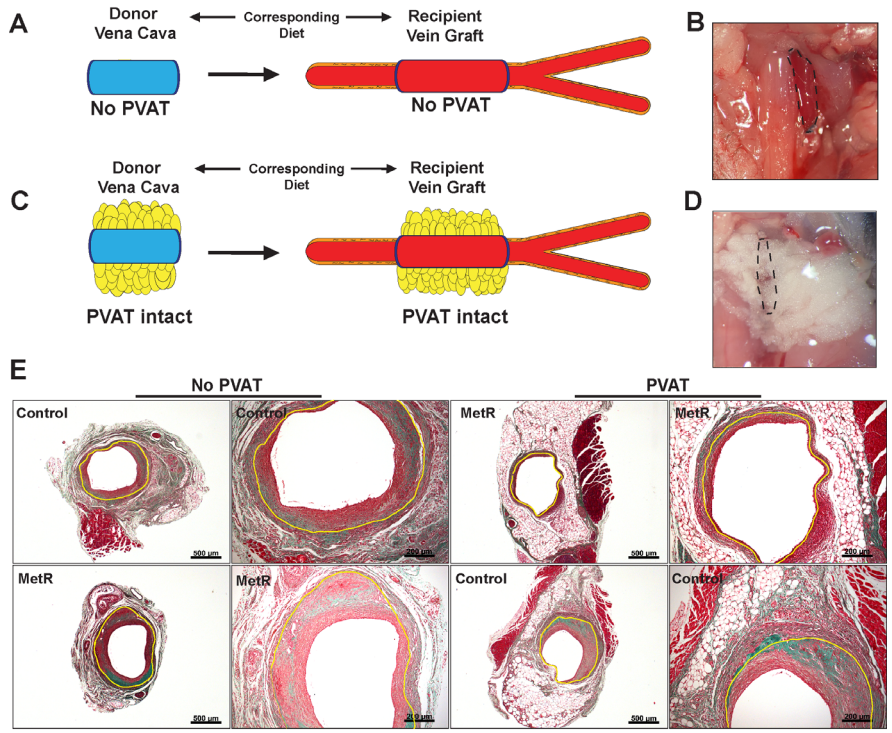

Figure 2. **Protection from Vein Graft Disease via Short-term Methionine Restriction is Perivascular Adipose Tissue Dependent. A-D:** schematic and in-situ images of vena cava/vein graft +- PVAT. **A**: stripping of vena cava PVAT results in vein graft lacking PVAT (**A-B**). **C**: vena cava with PVAT and consecutive vein graft with PVAT intact (**C-D**). **E**: Images of vein grafts at POD28 after Masson-trichome staining. Control-fed and MetR, no PVAT or PVAT. Scale bars 200μm or 500μm as indicated. **F-G**: histomorphometric analysis of POD28 vein grafts. **F**: I/M+A area ratio. **G**: I/M+A thickness ratio. **H:** M+A thickness. **F**: M+A area. All statistical testing was done via two-way ANOVA with Turkey's multiple comparisons test unless otherwise indicated, n=11-13/group. * P<0.05, ** P<0.01, *** P<0.001, **** P<0.0001

All data on the interaction between diet and PVAT on these histomorphometric parameters is summarized in **Table 1.** In conclusion, maximal protective effects of MetR on vein grafts were dependent on the interaction between PVAT surrounding the graft and MetR.

3.3 Favorable Vein Graft Wall Composition Seen in MetR Mice is Also Perivascular Adipose Tissue Dependent.

Because favorable vein graft adaptations upon MetR were mainly driven by alterations in outward layer (M+A) remodeling, we next examined how the diet-PVAT interaction impacted the cellular composition of the vein graft wall at POD28. Specifically in the MetR + PVAT group, reduced M_1/M_2-ratios were observed both in the graft wall (**Fig. 3A**) and PVAT (**Fig. 3B**). This favorable M_1/M_2 ratio present in both VG layers was driven by a significant interaction between MetR and the presence of PVAT (**Fig. 3A**, **Table 2)**. The observed differences in M_1/M_2-ratios could be explained by increased polarization towards the M_2-phenotype, both in the intimal/M+A layers (**Fig. 3C-D**) and in MetR PVAT (**Fig. S3A**), while there was a limited decrease in M_1-polarization in the vein graft wall (**Fig. 3C, 3E**) and PVAT (**Fig. S3B)**. Preconditioning with MetR yielded no difference in total M_θ macrophages in the vein graft wall (**Fig. S3C**), nor in surrounding PVAT (**Fig. S3D**). This increase in intimal M_2-macrophages together with an apparent small decrease in M_1-polarized macrophages in the MetR + PVAT cohort could also be linked to the underlying interplay between diet and PVAT (**Fig. 3D-E, Table 2**).

Also at POD28, percentage of intimal area and whole VG occupied by VSMC was dependent on the interaction between diet-PVAT (**Fig. 3F**, **Table 3**), but no significant difference in directionality could be detected between groups (**Fig. 3F**). The absolute number of VSMC per mm^2 present was comparably dependent on a combination of diet and PVAT, but this effect was not strong enough to display significant inter-group differences (**Fig. S3E**). There was no detectable change in proliferating VSMC at POD28 (**Fig. 3H**), nor did extra-cellular matrix analysis reveal a change in collagen deposition (**Fig. S3F**).

Together these data indicate that the interaction between MetR and PVAT prior to transplantation yielded a favorable remodeling phenotype of the graft at POD28, via increased M_2-macrophage polarization, correlating with a beneficial fibroproliferative response. Since mid- and long-term vein graft failure can be

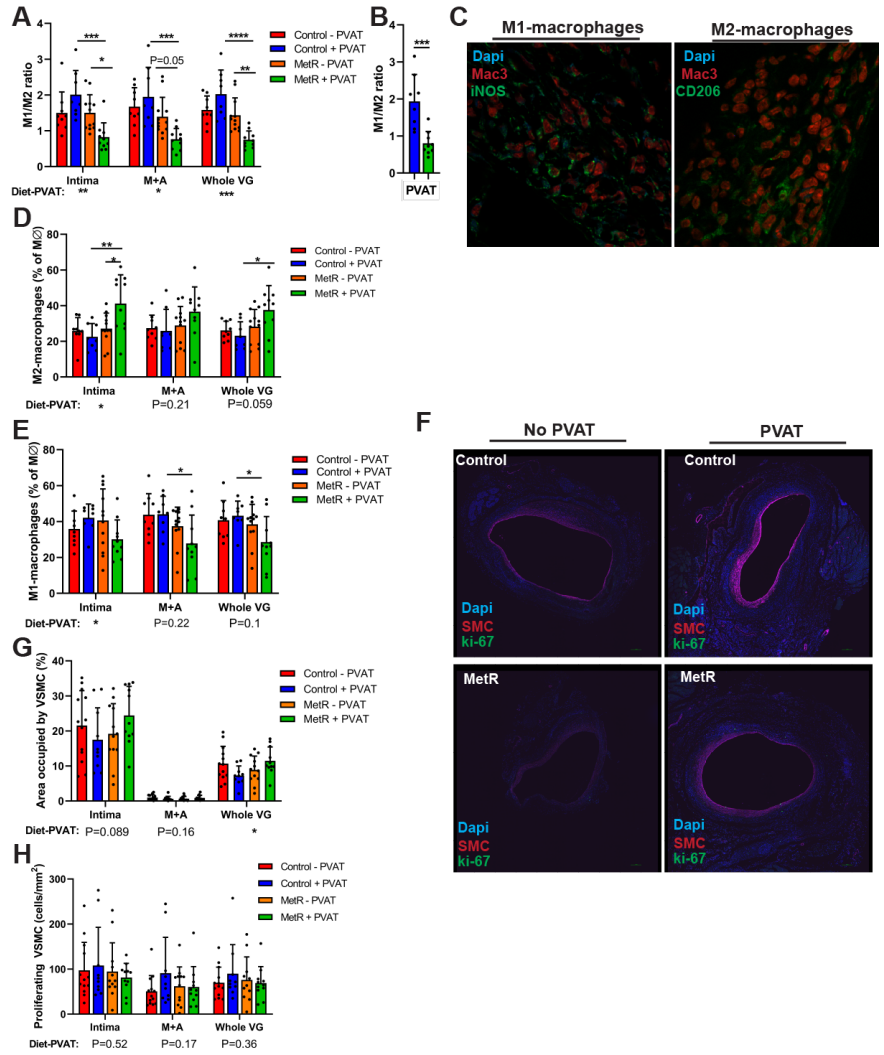

Figure 3. Favorable Vein Graft Wall Composition Seen in MetR Mice is Also Perivascular Adipose Tissue Dependent. A: M1/M2 ratio per vein graft layer. **B:** M1/M2 ratio in PVAT of MetR and control-fed mice. **C:** immunohistochemical staining for M1- and M2-macrophages. **D**: M2-macrophages as a percentage of total MΦ per vein graft layer. **E**: M1-macrophages as a percentage of total MΦ per vein graft layer. **F**: immunohistochemical staining for SMC-α and Ki-67. Scale bars = **G:** area occupied by VSMC per vein graft layer. **H:** proliferating VSMC (SMC-α + Ki-67 double positive cells) per mm^2 per vein graft layer. All statistical testing was done via two-way ANOVA with Tukey's multiple comparisons test, unless otherwise indicated, n=10-13/group. * P<0.05, ** P<0.01, *** P<0.001, **** P<0.0001.

Table 2. Percentage of variation between groups that can be explained by diet, PVAT or a diet-PVAT interaction. Two-way ANOVA with Tukey's multiple comparison test on M1/M2 ratio and M2-macrophages (left), M1-macrophages and MΦ macrophages (right). in **Figure 3** & **Fig. S3.** n=10-13/group.

Parameter	Source of Variation	% of total variation	P-value	P-value summary	Parameter	Source of Variation	% of total variation	P-value	P-value summary
M1/M2 ratio	Interaction	20.38	0.0016	**	M1-macrophages	Interaction	10.33	0.0489	*
Intima	PVAT +/-	0.3913	0.6384	ns	Intima	PVAT +/-	0.6856	0.6025	ns
(Fig. 3A)	Diet	20.11	0.0017	**	(Fig. 3E)	Diet	1.899	0.3876	ns
M1/M2 ratio	Interaction	10.70	0.018	*	M1-macrophages	Interaction	3.346	0.2238	ns
M+A	PVAT +/-	1.663	0.3345	ns	M+A	PVAT +/-	2.986	0.2500	ns
(Fig. 3A)	Diet	28.19	0.0003	***	(Fig. 3E)	Diet	17.65	0.0074	**
M/M2 ratio	Interaction	19.86	0.0006	***	M1-macrophages	Interaction	6.346	0.1039	ns
Whole VG	PVAT +/-	0.9584	0.4160	ns	Whole VG	PVAT +/-	2.260	0.3259	ns
(Fig. 3A)	Diet	31.89	<0.0001	****	(Fig. 3E)	Diet	11.99	0.0278	*
M2-macrophages	Interaction	12.01	0.0173	*	MΦ-macrophages	Interaction	20.02	0.0054	**
intima	PVAT +/-	4.668	0.1284	ns	intima	PVAT +/-	0.1291	0.8133	ns
(Fig. 3D)	Diet	15.95	0.0068	**	(Fig. S3F)	Diet	0.00009889	0.9948	ns
M2-macrophages	Interaction	4.024	0.2121	ns	MΦ-macrophages	Interaction	0.8676	0.5669	ns
M+A	PVAT +/-	1.793	0.4019	ns	M+A	PVAT +/-	0.2800	0.7446	ns
(Fig. 3D)	Diet	7.059	0.1012	ns	(Fig. S3F)	Diet	8.404	0.0806	ns
M2-Macrophages	Interaction	8.175	0.0594	ns	MΦ-macrophages	Interaction	0.4932	0.6300	ns
Whole VG	PVAT +/-	2.186	0.3205	ns	Whole VG	PVAT +/-	14.91	0.0113	*
(Fig. 3D)	Diet	14.73	0.0130	*	(Fig. S3F)	Diet	9.798	0.0372	*

traced back to temporal processes and adaptations immediately after graft implantation[9], we next evaluated baseline effects of MetR on PVAT and how this modulated vein graft PVAT during early remodeling.

3.4 Short-term MetR Modulates Caval Vein Perivascular Adipose Tissue Towards an Arterial-like Phenotype.

To delineate the effects of MetR on venous PVAT and to assess how MetR alters the response in PVAT to surgical injury (vein graft surgery), we performed transcriptomic analysis on caval vein PVAT and on PVAT from POD1 vein grafts (**Fig. S4A**). These baseline and early time points after surgery, when MetR diets were also halted, were chosen to test the hypothesis that the diet/adipose interaction was present at baseline, and capable of modulating the response during early vein graft remodeling. Thoracic aorta PVAT from control-fed and MetR mice was also sequenced to investigate arterial PVAT, which could not be harvested from RCCA due to technical limitations (**Fig. S4A**).

At baseline, venous (caval vein) PVAT from control-fed mice was distinct from arterial (aorta) PVAT (4568 genes, **Fig. 4A, D)**. Pathway analysis of these differentially expressed genes in arterial PVAT revealed a brown-adipose tissue like phenotype, with increased *thermogenesis* and *AMPK signaling* (**Fig. 4E)**. In arterial PVAT, MetR modified 1316 gene-transcripts (**Fig. 4B, D**) while further inducing *AMPK signaling* and *thermogenesis* pathways (**Fig. 4E**) compared to control-fed mice. In caval vein PVAT, MetR modified 811 different transcripts (**Fig. 4C**), including activation of *AMPK signaling* and *focal adhesion* pathways (**Fig. 4E**). Together, these data suggest that perivascular fat resembles BAT in terms of energy consumption rather than energy storage, and that MetR promotes this phenotype in both arterial and venous PVAT via canonical downstream activation of thermogenesis genes via AMPK[39] (**Fig. 4E**).

Analysis of PVAT at POD1 revealed vein graft surgery as a much larger modulator of gene expression than diet, with clear distinctions between baseline and POD1 in both diet groups, including 7492 and XXX? transcripts that were differentially regulated compared to baseline in control and MR groups, respectively (**Fig. 4F**). Despite the larger global effect of surgery, there were multiple differentially regulated genes as a function of diet on POD1 (**Fig. 4G**). Multiple pathways involved in PVAT energy-metabolism (AMPK signaling, fatty-acid biosynthesis) were differently regulated between diet groups in response to the surgery (**Fig. S4A-B)**. Next to regulation of energy storage and consumption genes, several pathways involved in the immune response showed an alternate response

between control and MetR, including hematopoietic linage (**Fig. S4C)**, primary immunodeficiency (**Fig. S4D**), B-cell receptor signaling (**Fig. S4E)** and toll like receptor signaling (**Fig. 4G**). Analysis of individual gene transcripts within these pathways revealed several differentially regulated transcripts in vein graft PVAT at POD1 as a result of MetR preconditioning. Among others, we observed a dampening of Tlr4 transcript expression (**Fig. S4H-I**) together with a robust decrease in transcripts for its endogenous ligand[40] tenascin-C (**Fig. 4I**) in the MetR group. Interestingly, the pro-atherosclerotic and pro-restenosis enzyme lysyl-oxidase[41] (LOX) was also strongly downregulated in MetR PVAT compared to control-fed at POD1 (**Fig. 4J**).

Table 3. Percentage of variation between groups that can be explained by diet, PVAT or a diet-PVAT interaction. Two-way ANOVA with Tukey's multiple comparison test on either % of vein graft layers occupied by VSMC, VSMC/mm^2, VSMC colocalizing with Ki-67 or % of vein graft layers occupied by collagen. As depicted in graphs in **Figure 3** & **Fig. S3.** n=10-13/group.

Parameter	Source of Variation	% of total variation	P-value	P-value summary	Parameter	Source of Variation	% of total variation	P-value	P-value summary
% VSMC of	Interaction	6.622	0.0897	ns	VSMC/mm^2	Interaction	4.246	0.1832	ns
Intima (Fig. 3G)	PVAT +/- Diet	0.1041 1.583	0.8286 0.4005	ns ns	Intima (Fig. S3E)	PVAT +/- Diet	0.008998 1.033	0.9506 0.5080	ns ns
% VSMC of	Interaction	4.430	0.1693	ns	VSMC/mm^2	Interaction	6.810	0.0860	ns
M+A	PVAT +/-	0.1700	0.7855	ns	M+A	PVAT +/-	1.037	0.4962	ns
(Fig. 3G)	Diet	0.1062	0.8296	ns	(Fig. S3E)	Diet	1.278	0.4504	ns
% VSMC of	Interaction	13.01	0.0153	*	VSMC/mm^2	Interaction	10.20	0.0355	*
Whole VG	PVAT +/-	0.2532	0.7262	ns	Whole VG	PVAT +/-	1.095	0.4802	ns
(Fig. 3G)	Diet	2.068	0.3194	ns	(Fig. S3E)	Diet	0.4385	0.6545	ns
VSMC+ Ki-67	Interaction	0.9706	0.5219	ns	% collagen of	Interaction	2.705	0.2627	ns
intima	PVAT +/-	0.01213	0.9428	ns	Intima	PVAT +/-	1.738	0.3681	ns
(Fig. 3H)	Diet	1.456	0.4334	ns	(Fig. S3E)	Diet	3.099	0.2311	ns
VSMC+ Ki-67	Interaction	4.180	0.1743	ns	% collagen of	Interaction	0.05245	0.8773	ns
M+A	PVAT +/-	3.468	0.2151	ns	M+A	PVAT +/-	1.229	0.4562	ns
(Fig. 3H)	Diet	0.8681	0.5323	ns	(Fig. S3E)	Diet	2.802	0.2625	ns
VSMC+ Ki-67	Interaction	2.150	0.3458	ns	% collagen of	Interaction	0.7912	0.5427	ns
Whole VG	PVAT +/-	0.5066	0.6458	ns	Whole VG	PVAT +/-	2.748	0.2591	ns
(Fig. 3H)	Diet	0.6122	0.6135	ns	(Fig. S3E)	Diet	3.815	0.1848	ns

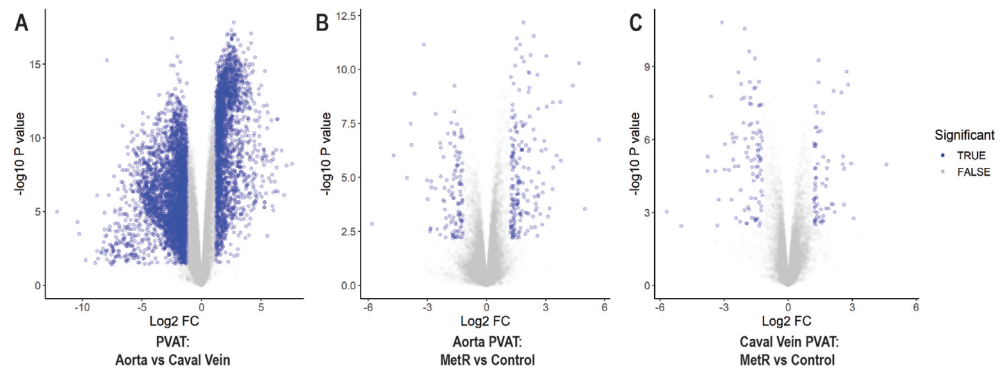

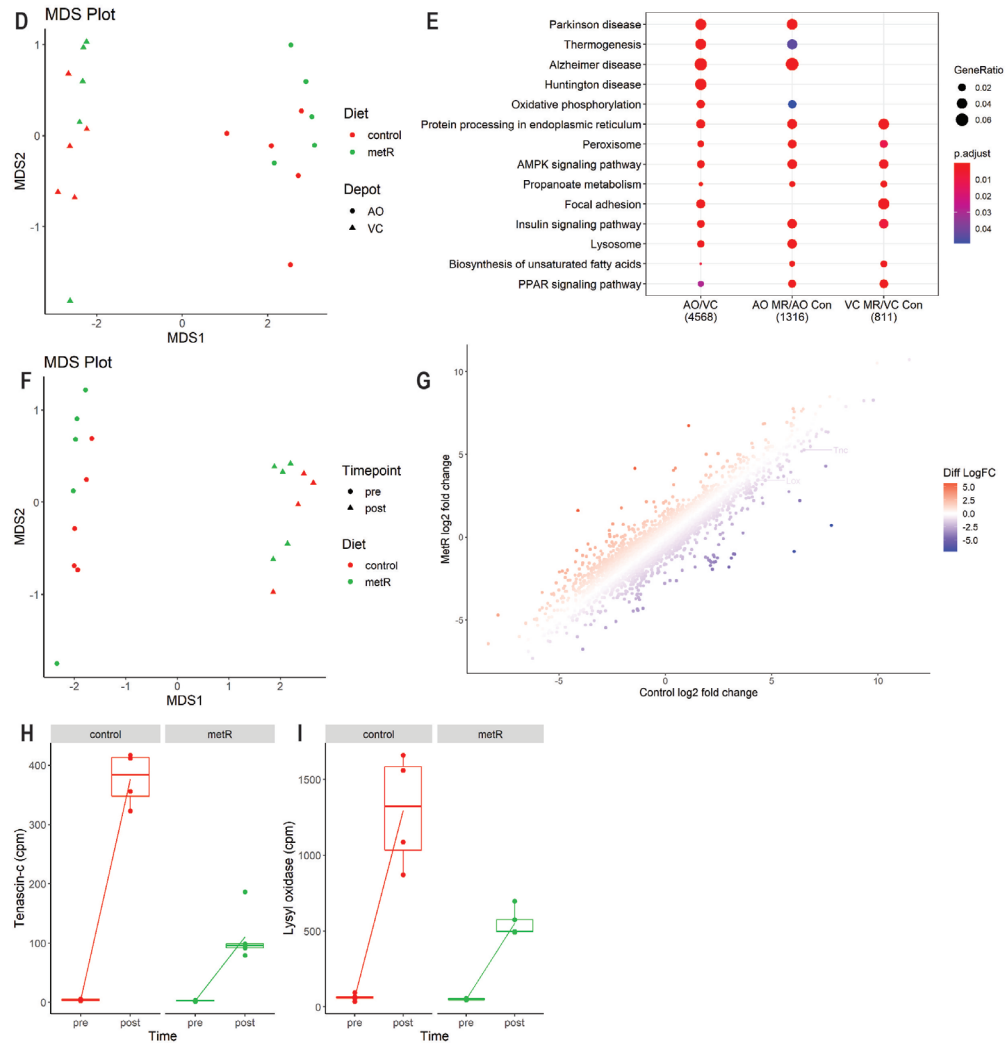

Figure 4. Short-term MetR Modulates Caval Vein Perivascular Adipose Tissue Towards an Arterial-like Phenotype and Dampens Post-op Inflammation A: fold change in transcript expression in control-fed aorta PVAT versus control-fed caval vein PVAT. **B**: fold change in transcript expression in aorta PVAT of MetR versus control-fed mice. **C**: fold change in transcript expression in caval vein PVAT of MetR versus control-fed mice. **D**: principal component analysis of aorta and caval vein PVAT of control-fed and MetR mice. **E**: pathway analysis of aorta versus caval vein PVAT of control-fed mice (AO/VC, first column), aorta PVAT MetR versus control-fed (AO MR/AO Con, second column) and caval vein PVAT MetR versus control-fed (VC MR/ VC Con, third column). **F**: principal component analysis of control-fed and MetR PVAT from caval vein and POD1 vein grafts. **G**: fold change in transcript expression between caval vein PVAT and vein graft PVAT at POD1 for both control-fed and MetR mice. **H**: tenascin-c transcript expression (in counts per million) in control-fed and MetR mice caval vein and vein graft PVAT. **I**: lysyl oxidase transcript expression (in counts per million) in control-fed and MetR mice caval vein and vein graft PVAT.

4. Discussion.

In this current study, we tested the potential of short-term dietary restriction of the sulfur amino-acids methionine and cysteine, in cardiovascular surgery preclinical models. This MetR intervention, which constitutes an isocaloric diet with adequate levels of all macronutrients, protected from arterial IH in a focal stenosis model, and improved vein graft adaptation to an arterial circulation in a model of bypass surgery. Specifically, in bypass surgery, MetR further improved graft remodeling when the donor caval vein was implanted with PVAT intact. Control-fed mice who received a caval vein with intact PVAT had exacerbated VGD at POD28, pointing towards a diet-induced reversal of PVAT phenotype in MetR mice compared to control diet. There was no significant histomorphometric difference detectable between diet groups when caval veins were stripped of PVAT before anastomosis creation, suggestive of a PVAT-dependent protection from VGD yielded by MetR.

Whether protection from VGD is conferred via MetR in the donor or recipient mouse, or whether this concerns an interplay between local PVAT phenotype and systemic (recipient) effects of diet remains unclear. Recently we found that a short-term reduction of total proteins before vein graft surgery protects from VGD.[27] There, we also tested whether protection originated from protein restriction in either the donor or the recipient and found that recipient-only restriction was adequate for protection and that this was enhanced when utilizing both donor and recipients on protein restriction diets. Simultaneously, donor-only restriction was not, which appears to contradict our current findings on the importance of donor PVAT. However, in that study and in our initial MetR vein graft study (**Fig. 1E-H**), we partially stripped the caval vein of its PVAT. This could account for both the apparent inability of donor-only restriction to yield protection in our previous study, as well as the difference in effect-size after MetR between **Fig. 1E-H** and **Fig. 2F-G**.

Our in-depth analysis and side-by-side comparison of arterial and venous PVAT revealed a distinct transcriptomic profile between vein and artery PVAT, with venous PVAT resembling white/beige adipose tissue.[42] Arterial PVAT closely resembled BAT, as seen by the presence of several genes involved in thermogenesis and in accordance with previous studies.[43] Preconditioning with MetR further upregulated thermogenesis gene transcripts, together with an increase in upstream AMPK-signaling. In venous PVAT, although thermogenesis was not increased, AMPK signaling was up, suggestive of browning of this white/beige adipose tissue depot.

Here we show that short-term MetR attenuates VGD, and that this effect is dependent on intact vein PVAT during implantation. MetR activated both venous and arterial PVAT AMPK signaling and consequently browning in arterial and possibly venous PVAT. Suggestive of caval vein PVAT with a BAT/arterial PVAT signature after MetR, which could explain (part) of the protection from VGD after MetR. Follow-up studies should determine the cell types involved in protection from VGD by MetR. Furthermore, donor vs recipient and immune-cell labeling could determine the mechanistic interplay between MetR, donor PVAT and the recipients local and systemic characteristics that together attenuate VGD.

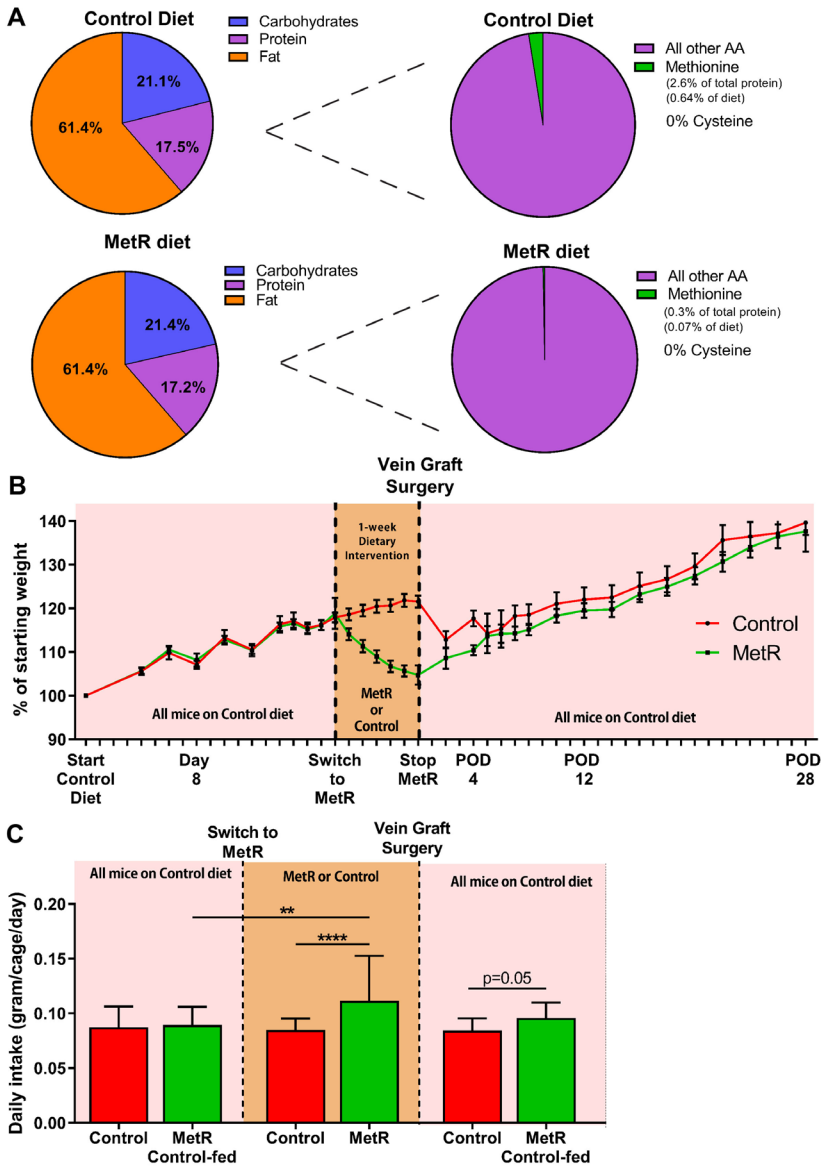

Supplemental figure 1. Methionine restriction diet composition and metabolic response. A: Macronutrient composition of control and methionine restricted diet. Both diets contain 0% cysteine and 60% fat. **B:** representative graph of percentage of starting weight that was lost/gained during the study. **C**: representative bar graph of daily food-intake during study in both groups. ** P<0.01, **** P<0.0001. All statistical testing was done via two-way ANOVA with Turkey's multiple comparisons test, unless otherwise indicated.

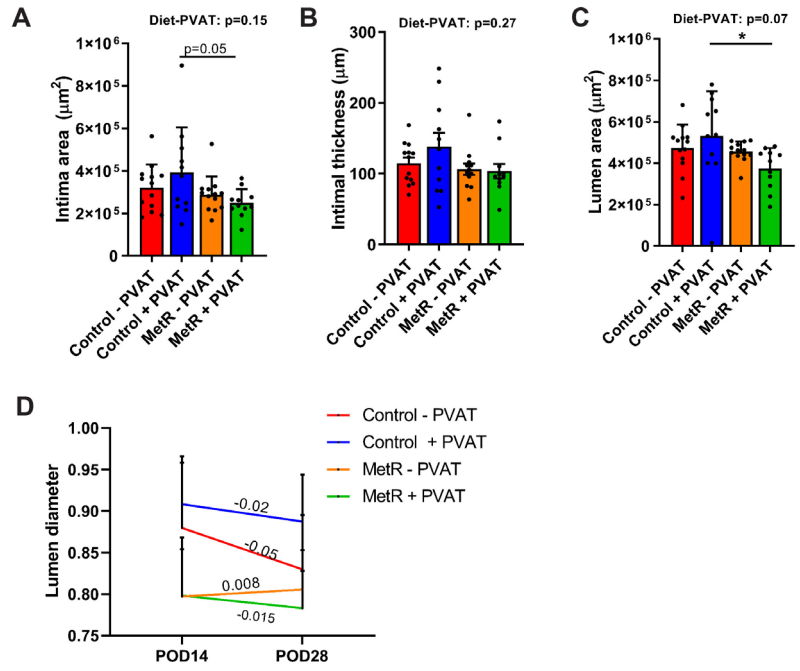

Supplemental figure 2. Intimal area/thickness and lumen diameters at POD28. A-C: Histomorphometric analysis of vein grafts at POD28. **A**: Intimal area. **B**: Intimal thickness. **C:** Lumen area. **D**: Lumen diameter ultrasound measurements at POD14 and POD28, with rate of lumen increase/decrease. All statistical testing was done via two-way ANOVA with Tukey's multiple comparison's test unless otherwise indicated, n=11-13/group. * P<0.05

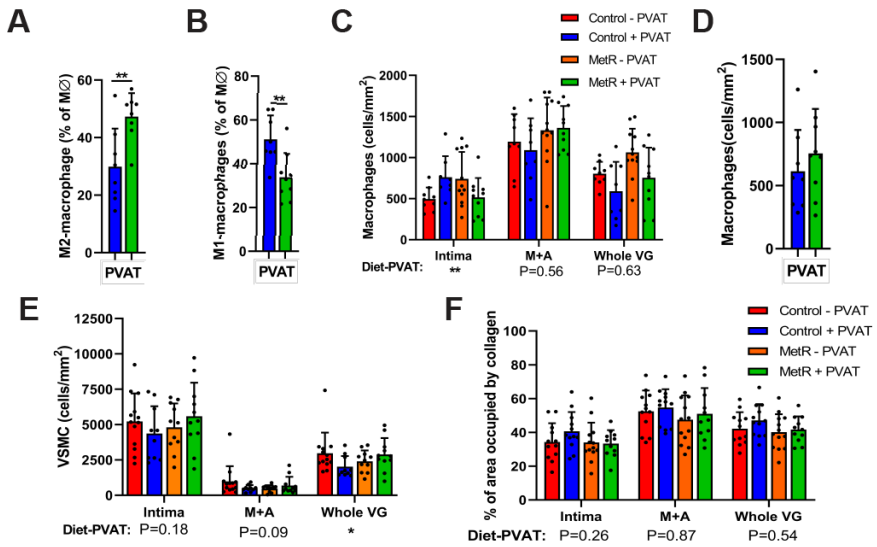

Supplemental figure 3. VSMC density, collagen content and MΦ macrophages in Vein Grafts and PVAT at POD28. A: M_2-macrophage count in PVAT of control-fed and MetR mice, in cells/mm^2. **B**: M_1-macrophage count in PVAT of control-fed and MetR mice, in cells/mm^2. C: MΦ-macrophages per vein graft layer in cells/mm^2. **D**: MΦ-macrophage count in PVAT of control-fed and MetR mice, in cells/mm^2. **E**: VSMC density per vein graft layer in cells/mm^2. **F**: percentage of vein graft layer occupied by collagen. All statistical testing was done via two-way ANOVA with Tukey's multiple comparisons test, unless indicated otherwise, n=10-13/group. ** P<0.01.

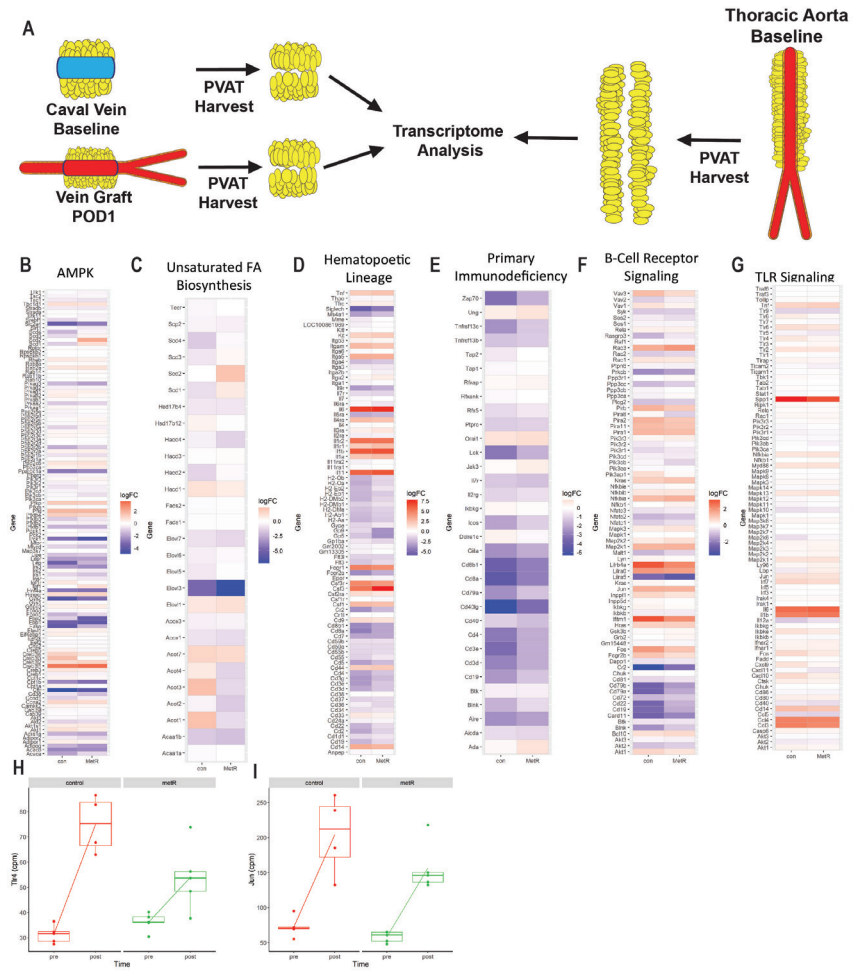

Supplemental figure 4. Transcriptome analysis of control-fed and MetR PVAT. A: schematic of caval vein and vein graft POD1 PVAT; and of thoracic aorta PVAT harvest, three separate adipose tissue depots processed for transcriptome analysis simultaneously. **B-G**: gene-patway heatmaps for control and MetR-fed mice, fold change between baseline versus POD1. **B**: AMPK-pathway gene heatmap. **C**: Unsaturated fatty-acid biosynthesis. **D**: Hematopoetic lineage pathway. **E:** Primary Immunodeficiency. **F:** B-cell receptor signaling. **G: F-H**: expression of tlr4 and jun transcipts (in counts per million) in caval vein and vein graft PVAT from control-fed and MetR mice.

5. References.

1. Jim J, Owens PL, Sanchez LA and Rubin BG. Population-based analysis of inpatient vascular procedures and predicting future workload and implications for training. *J Vasc Surg*. 2012;55:1394-9; discussion 1399-400.
2. Virani SS, Alonso A, Benjamin EJ, Bittencourt MS, Callaway CW, Carson AP, Chamberlain AM, Chang AR, Cheng S, Delling FN, Djousse L, Elkind MSV, Ferguson JF, Fornage M, Khan SS, Kissela BM, Knutson KL, Kwan TW, Lackland DT, Lewis TT, Lichtman JH, Longenecker CT, Loop MS, Lutsey PL, Martin SS, Matsushita K, Moran AE, Mussolino ME, Perak AM, Rosamond WD, Roth GA, Sampson UKA, Satou GM, Schroeder EB, Shah SH, Shay CM, Spartano NL, Stokes A, Tirschwell DL, VanWagner LB and Tsao CW. Heart Disease and Stroke Statistics-2020 Update: A Report From the American Heart Association. *Circulation*. 2020;141:e139-e596.
3. Krankenberg H, Schlüter M, Steinkamp HJ, Bürgelin K, Scheinert D, Schulte KL, Minar E, Peeters P, Bosiers M, Tepe G, Reimers B, Mahler F, Tübler T and Zeller T. Nitinol stent implantation versus percutaneous transluminal angioplasty in superficial femoral artery lesions up to 10 cm in length: the femoral artery stenting trial (FAST). *Circulation*. 2007;116:285-92.
4. Laird JR, Katzen BT, Scheinert D, Lammer J, Carpenter J, Buchbinder M, Dave R, Ansel G, Lansky A, Cristea E, Collins TJ, Goldstein J and Jaff MR. Nitinol stent implantation versus balloon angioplasty for lesions in the superficial femoral artery and proximal popliteal artery: twelve-month results from the RESILIENT randomized trial. *Circulation Cardiovascular interventions*. 2010;3:267-76.
5. Zhao Q, Zhu Y, Xu Z, Cheng Z, Mei J, Chen X and Wang X. Effect of Ticagrelor Plus Aspirin, Ticagrelor Alone, or Aspirin Alone on Saphenous Vein Graft Patency 1 Year After Coronary Artery Bypass Grafting: A Randomized Clinical Trial. *Jama*. 2018;319:1677-1686.
6. Conte MS, Bandyk DF, Clowes AW, Moneta GL, Seely L, Lorenz TJ, Namini H, Hamdan AD, Roddy SP, Belkin M, Berceli SA, DeMasi RJ, Samson RH and Berman SS. Results of PREVENT III: A multicenter, randomized trial of edifoligide for the prevention of vein graft failure in lower extremity bypass surgery. *Journal of Vascular Surgery*. 2006;43:742-751.e1.
7. Yahagi K, Kolodgie FD, Otsuka F, Finn AV, Davis HR, Joner M and Virmani R. Pathophysiology of native coronary, vein graft, and in-stent atherosclerosis. *Nat Rev Cardiol*. 2016;13:79-98.
8. de Vries MR and Quax PHA. Inflammation in Vein Graft Disease. *Frontiers in cardiovascular medicine*. 2018;5:3.
9. de Vries MR, Simons KH, Jukema JW, Braun J and Quax PHA. Vein graft failure: from pathophysiology to clinical outcomes. *Nat Rev Cardiol*. 2016;13:451-470.
10. Brown NK, Zhou Z, Zhang J, Zeng R, Wu J, Eitzman DT, Chen YE and Chang L. Perivascular adipose tissue in vascular function and disease: a review of current research and animal models. *Arterioscler Thromb Vasc Biol*. 2014;34:1621-30.
11. Fernández-Alfonso MS, Gil-Ortega M, Aranguez I, Souza D, Dreifaldt M, Somoza B and Dashwood MR. Role of PVAT in coronary atherosclerosis and vein graft patency: friend or foe? *British journal of pharmacology*. 2017;174:3561-3572.
12. Chatterjee TK, Stoll LL, Denning GM, Harrelson A, Blomkalns AL, Idelman G, Rothenberg FG, Neltner B, Romig-Martin SA, Dickson EW, Rudich S and Weintraub NL. Proinflammatory phenotype of perivascular adipocytes: influence of high-fat feeding. *Circulation research*. 2009;104:541-9.
13. MR S, N E, S H, I J, M L-N, FS C, G C, S K and K S. Leptin-dependent and leptin-independent paracrine effects of perivascular adipose tissue on neointima formation. *Arterioscler Thromb Vasc Biol*. 2013;33:980-7.
14. Manka D, Chatterjee T, Stoll L, Basford J, Konaniah E, Srinivasan R, Bogdanov V, Tang Y, Blomkalns A, Hui D and Weintraub N. Transplanted Perivascular Adipose Tissue Accelerates Injury-Induced Neointimal Hyperplasia: Role of Monocyte Chemoattractant Protein-1. *Arterioscler Thromb Vasc Biol*. 2014;34:1723-1730.
15. Longchamp A, Tao M, Bartelt A, Ding K, Lynch L, Hine C, Corpataux JM, Kristal BS, Mitchell JR and Ozaki CK. Surgical injury induces local and distant adipose tissue browning. *Adipocyte*. 2016;5:163-74.
16. Pachler C, Ikeoka D, Plank J, Weinhandl H, Suppan M, Mader JK, Bodenlenz M, Regittnig W, Mangge H, Pieber TR and Ellmerer M. Subcutaneous adipose tissue exerts proinflammatory cytokines after minimal trauma in humans. *American journal of physiology*. 2007;293:E690-6.
17. Gletsu N, Lin E, Zhu JL, Khaitan L, Ramshaw BJ, Farmer PK, Ziegler TR, Papanicolaou DA and Smith CD. Increased plasma interleukin 6 concentrations and exaggerated adipose tissue interleukin 6 content in severely obese patients after operative trauma. *Surgery*. 2006;140:50-7.
18. Nguyen B, Tao M, Yu P, Mauro C, Seidman MA, Wang YE, Mitchell J and Ozaki CK. Pre-Operative Diet Impacts the Adipose Tissue Response to Surgical Trauma. *Surgery*. 2013;153:584-593.
19. Mitchell JR, Verweij M, Brand K, van de Ven M, Goemaere N, van den Engel S, Chu T, Forrer F, Müller C, de Jong M, van Ijcken W, Ijzermans JNM, Hoeijmakers JHJ and de Bruin RWF. Short-term dietary restriction and fasting precondition against ischemia reperfusion injury in mice. *Aging cell*. 2010;9:40-53.
20. Mitchell JR, Beckman JA, Nguyen LL and Ozaki CK. Reducing elective vascular surgery perioperative risk with brief preoperative dietary restriction. *Surgery*. 2013.
21. Longchamp A, Harputlugil E, Corpataux JM, Ozaki CK and Mitchell JR. Is Overnight Fasting before Surgery Too Much or Not Enough? How Basic Aging Research Can Guide Preoperative Nutritional Recommendations to Improve Surgical Outcomes: A Mini-Review. *Gerontology*. 2017;63:228-237.
22. Robertson LT, Treviño-Villarreal JH, Mejia P, Grondin Y, Harputlugil E, Hine C, Vargas D, Zheng H, Ozaki CK, Kristal BS, Simpson SJ and Mitchell JR. Protein and Calorie Restriction Contribute Additively to Protection from Renal Ischemia Reperfusion Injury Partly via Leptin Reduction in Male Mice. *The Journal of nutrition*. 2015;145:1717-1727.
23. Hine C, Harputlugil E, Zhang Y, Ruckenstuhl C, Lee BC, Brace L, Longchamp A, Trevino-Villarreal JH, Mejia P, Ozaki CK, Wang R, Gladyshev VN, Madeo F, Mair WB and Mitchell JR. Endogenous Hydrogen Sulfide Production Is Essential for Dietary Restriction Benefits. *Cell*. 2015;160:132-144.
24. Verweij M, van Ginhoven TM, Mitchell JR, Sluiter W, van den Engel S, Roest HP, Torabi E, Ijzermans JN, Hoeijmakers JH and de Bruin RW. Preoperative fasting protects mice against hepatic ischemia/reperfusion injury: mechanisms and effects on liver regeneration. *Liver transplantation: official publication of the American Association for the Study of Liver Diseases and the International Liver Transplantation Society*. 2011;17:695-704.
25. Hine C and Mitchell JR. Calorie restriction and methionine restriction in control of endogenous hydrogen sulfide production by the transsulfuration pathway. *Experimental gerontology*. 2014.

26. Mauro CR, Tao M, Yu P, Trevino-Villerreal JH, Longchamp A, Kristal BS, Ozaki CK and Mitchell JR. Preoperative dietary restriction reduces intimal hyperplasia and protects from ischemia-reperfusion injury. *J Vasc Surg*. 2014.
27. Trocha KM, Kip P, Tao M, MacArthur MR, Trevino-Villarreal JH, Longchamp A, Toussaint W, Lambrecht BN, de Vries MR, Quax PHA, Mitchell JR and Ozaki CK. Short-term preoperative protein restriction attenuates vein graft disease via induction of cystathionine gamma-lyase. *Cardiovasc Res*. 2020;116:416-428.
28. Orgeron ML, Stone KP, Wanders D, Cortez CC, Van NT and Gettys TW. The impact of dietary methionine restriction on biomarkers of metabolic health. *Prog Mol Biol Transl Sci*. 2014;121:351-376.
29. Orentreich N, Matias JR, DeFelice A and Zimmerman JA. Low methionine ingestion by rats extends life span. *J Nutr*. 1993;123:269-74.
30. Perrone CE, Mattocks DA, Plummer JD, Chittur SV, Mohney R, Vignola K, Orentreich DS and Orentreich N. Genomic and metabolic responses to methionine-restricted and methionine-restricted, cysteine-supplemented diets in Fischer 344 rat inguinal adipose tissue, liver and quadriceps muscle. *Journal of nutrigenetics and nutrigenomics*. 2012;5:132-57.
31. Patil YN, Dille KN, Burk DH, Cortez CC and Gettys TW. Cellular and molecular remodeling of inguinal adipose tissue mitochondria by dietary methionine restriction. *The Journal of nutritional biochemistry*. 2015;26:1235-47.
32. Longchamp A, Mirabella T, Arduini A, MacArthur MR, Das A, Treviño-Villarreal JH, Hine C, Ben-Sahra I, Knudsen NH, Brace LE, Reynolds J, Mejia P, Tao M, Sharma G, Wang R, Corpataux J-M, Haefliger J-A, Ahn KH, Lee C-H, Manning BD, Sinclair DA, Chen CS, Ozaki CK and Mitchell JR. Amino Acid Restriction Triggers Angiogenesis via GCN2/ATF4 Regulation of VEGF and H2S Production. *Cell*. 2018;173:117-129.e14.
33. Trocha K, Kip P, MacArthur MR, Mitchell SJ, Longchamp A, Treviño-Villarreal JH, Tao M, Bredella MA, De Amorim Bernstein K, Mitchell JR and Ozaki CK. Preoperative Protein or Methionine Restriction Preserves Wound Healing and Reduces Hyperglycemia. *Journal of Surgical Research*. 2019;235:216-222.
34. Plaisance EP, Greenway FL, Boudreau A, Hill KL, Johnson WD, Krajcik RA, Perrone CE, Orentreich N, Cefalu WT and Gettys TW. Dietary methionine restriction increases fat oxidation in obese adults with metabolic syndrome. *The Journal of clinical endocrinology and metabolism*. 2011;96:E836-40.
35. Tao M, Mauro CR, Yu P, Favreau JT, Nguyen B, Gaudette GR and Ozaki CK. A simplified murine intimal hyperplasia model founded on a focal carotid stenosis. *Am J Pathol*. 2013;182:277-87.
36. Wezel A, de Vries MR, Maassen JM, Kip P, Peters EA, Karper JC, Kuiper J, Bot I and Quax PHA. Deficiency of the TLR4 analogue RP105 aggravates vein graft disease by inducing a pro-inflammatory response. *Scientific reports*. 2016;6:24248.
37. Yu P, Nguyen BT, Tao M, Bai Y and Ozaki CK. Mouse Vein Graft Hemodynamic Manipulations to Enhance Experimental Utility. *The American Journal of Pathology*. 2011;178:2910-2919.
38. Zhang L, Hagen PO, Kisslo J, Peppel K and Freedman NJ. Neointimal hyperplasia rapidly reaches steady state in a novel murine vein graft model. *J Vasc Surg*. 2002;36:824-32.
39. Wu L, Zhang L, Li B, Jiang H, Duan Y, Xie Z, Shuai L, Li J and Li J. AMP-Activated Protein Kinase (AMPK) Regulates Energy Metabolism through Modulating Thermogenesis in Adipose Tissue. *Frontiers in physiology*. 2018;9:122.
40. Goh FG, Piccinini AM, Krausgruber T, Udalova IA and Midwood KS. Transcriptional regulation of the endogenous danger signal tenascin-C: a novel autocrine loop in inflammation. *J Immunol*. 2010;184:2655-62.
41. Rodríguez C, Martínez-González J, Raposo B, Alcudia JF, Guadall A and Badimon L. Regulation of lysyl oxidase in vascular cells: lysyl oxidase as a new player in cardiovascular diseases. *Cardiovasc Res*. 2008;79:7-13.
42. van Dam AD, Boon MR, Berbée JFP, Rensen PCN and van Harmelen V. Targeting white, brown and perivascular adipose tissue in atherosclerosis development. *European journal of pharmacology*. 2017;816:82-92.
43. Fitzgibbons TP, Kogan S, Aouadi M, Hendricks GM, Straubhaar J and Czech MP. Similarity of mouse perivascular and brown adipose tissues and their resistance to diet-induced inflammation. *Am J Physiol Heart Circ Physiol*. 2011;301:H1425-37.